EQCM study of anomalous Zn–Ni codeposition in acid sulfate electrolyte

Renata Valotkienė, Konstantinas Leinartas, Dalia Virbalytė and Eimutis Juzeliūnas

Institute of Chemistry, A. Goštauto 9, LT-2600 Vilnius, Lithuania

The initial stages of Zn–Ni electrodeposition were investigated by electrochemical quartz crystal microbalance. The mass change dependencies recorded in the region of anomalous codeposition under constant current or constant potential conditions exhibited three distinctive regions: 1) the initial mass growth, which was much higher than that predicted by Faraday's law and was attributed to precipitation of hydroxides on the surface; 2) a decrease in mass due to hydrogen evolution, and 3) a rectilinear increase in mass due to alloy deposition. Such a behavior was explained in terms of the so-called hydroxide suppression mechanism, which explains anomalous zinc codeposition with iron group metals. The reported data are in agreement with the EQCM results obtained previously for Zn–Co anomalous codeposition.

Key words: zinc, nickel, alloy, interphase layer, quartz crystal microgravimetry, anomalous codeposition

INTRODUCTION

Investigations of codeposition of iron group metals with zinc have attracted considerable attention in the last decade because of an exceptional technological significance of Zn–Ni, Zn–Co and Zn–Fe alloys. It is common knowledge that the corrosion resistance of these alloys is significantly higher than that of pure zinc. In spite of numerous investigations of Zn–Ni alloy deposition [1–21], the mechanism of the process is not well understood. Electrochemical codeposition of zinc with nickel is known as anomalous one, because reduction of the less noble zinc is preferential. The existing interpretations of the anomalous codeposition are equivocal. An underpotential deposition hypothesis was proposed in [22], according to which the deposition proceeds continuously on a surface which is different from the parent metals, and therefore deposition of the less noble component is preferential. Ohtsuka and Komori have recently supported the underpotential deposition mechanism by the information obtained using *in situ* ellipsometry [1]. Mathias and Chapman [2, 3] and Landolt [4] attributed anomalous codeposition to different kinetic behaviour of both components. Interaction of Ni and Zn nuclei with developed hydrogen was concluded to be responsible for preferential Zn deposition [5, 6]. An inhibiting deposition of the alloying additive was explained in terms of the retardation effect of zinc hydroxide phase included in the alloy matrix [7]. Authors of [8] suggested that an intermediate $(NiZn)^{+}_{ads}$ forms during alloy deposition, which is a cause of anomalous codeposition. It has been found in [9] that anomalous Zn–Ni codeposition occurred only in the far cathodic region of the voltammetric curve, where intensive hydrogen evolution took place. In contrast to normal codeposition, the anomalous one was not influenced by mass transport rate.

The hydroxide suppression mechanism (HSM) was suggested by Dahms and Croll in their discussion of iron-nickel anomalous codeposition [23]. This mechanism was suggested also for zinc–cobalt and zinc–nickel codeposition by other authors [24–26]. The HSM implies a rise in pH in the vicinity of the cathode during electrolysis and precipitation of a zinc hydroxide film, which prevents deposition of the nobler component. The suggestion of the precipitation of zinc hydroxide was supported also by the results obtained using electrochemical quartz crystal microbalance (EQCM) [10]. By EQCM an anomalously high mass growth was detected in the initial stages of Zn–Co deposition, which was explained in terms of precipitation of zinc hydroxide on the surface. A strongly suppressed nickel codeposition in acetate bath was also explained by formation and adsorption of zinc hydroxide on the electrode [11].

Hence, interpretations of anomalous Zn–Ni codeposition are equivocal, and therefore additional experimental data are needed to support any of the

proposed mechanisms. In the present study, Zn–Ni deposition was examined by EQCM. This *in situ* technique, due to high sensitivity to mass changes, is capable of providing important information about hydroxide precipitation, hydrogen evolution and alloy deposition.

EXPERIMENTAL

The plating bath contained 0.84 M $ZnSO_4 \cdot 7H_2O$ and 1.36 M $NiSO_4 \cdot 6H_2O$. The solution was acidified to pH 1.6 by H_2SO_4. The reagents of analytical class purity and triply distilled water were used to prepare the plating bath.

The working electrode was made of gold in a Teflon frame. The working surface was 0.78 cm^2. The reference electrode was a saturated Ag/AgCl electrode, and platinum foil served as a counter electrode.

The voltammetric measurements were performed by using a PS-305 potentiostat from Elchema (USA) in a standard three-electrode one-compartment glass cell. The solution temperature was maintained by a thermostat at 25 °C.

EQCM measurements were conducted using quartz discs produced by Quartzverarbeitung (Germany), their fundamental frequency being f_o = 5 MHz and d = 15 mm. Both quartz sides were plated with gold 200 nm thick using the standard vacuum thermal evaporation technique. The geometric area of the working electrode was 0.78 cm^2. According to [27], a theoretical proportion coefficient between changes in quartz oscillation frequency and added electrode mass is 18 ng Hz^{-1} cm^{-2}, when the main resonance frequency is f_o= 5 MHz. The EQCM device used has been described elsewhere [28].

The nickel content in the alloy was determined by atomic absorption spectroscopy after dissolution of the coatings in hydrochloric acid. A Perkin-Elmer 603 machine has been used for analysis.

RESULTS AND DISCUSSION

Figure 1 shows potential *vs*. current density dependencies recorded using a gold electrode in solutions containing Ni^{++}, Zn^{++} and the both. Marked cathodic currents appear below *ca*. –0.5 V, and limiting currents are observed in all solutions in appropriate potential regions.

Coating compositions deposited at different potentials are shown in Table 1.

Let us remember that the molar ratio [Ni^{++}]/[Zn^{++}] in the solution is 1.45. Comparing this value to the analogous one in the coatings, we can see that anomalous Zn–Ni deposition takes place at –0.9 V, –0.98 and –1.18 V, while deposition at potentials –0.5, –0.6, –0.68, –0.77 and –0.85 V is normal. Thus, anomalous codeposition is favoured at a higher cathodic polarisation. The normal deposition change to anomalous one with a decrease in electrode potential has been observed also by other authors [9].

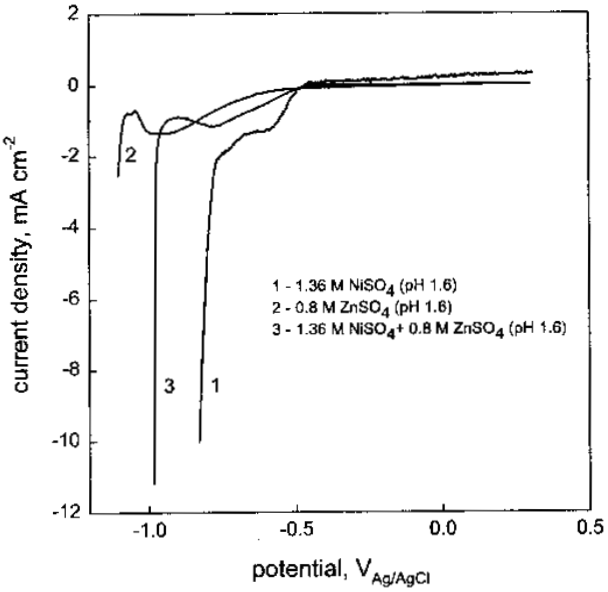

Fig. 1. Potentiodynamic voltammetric dependencies obtained using gold electrode at potential sweep rate 5 mv/s in the solutions: 1.36 M $NiSO_4$ (*1*), 0.8 M $ZnSO_4$ (*2*) and 1.36 M $NiSO_4$ + 0.8 M $ZnSO_4$ (*3*). The solutions have been adjusted to pH 1.6

Table. 1. **Molar ratio Ni/Zn in the coatings obtained at different electrode polarizations in 0.84 M $ZnSO_4$ and 1.36 M $NiSO_4$ solution (pH = 1.6)**

E, $V_{Ag/AgCl}$	–0.5	–0.6	–0.68	–0.77	–0.85	–0.9	–0.98	–1.18
[Ni]/[Zn]	1.77	2.33	3.74	1.96	1.35	0.7	0.26	0.13

Prior to the study of the alloy deposition by EQCN, one has to reveal the microgravimetric behaviour in a blank supporting solution, where the only possible faradaic process is hydrogen evolution. Figure 2 shows mass *vs*. time change when the cathodic current has been switched on in the Na_2SO_4 solution adjusted to pH 1.6. A slight increase in electrode mass (ca. 200 ng/cm^2) was observed immediately after the cathodic current had been applied. This increase may be ascribed to adsorption of hydrogen atoms on the electrode and bonding of water molecules with the surface via these hydrogen atoms. Consequently, the surface becomes more hydrophilic, *i.e*. develops a thicker adhering solution layer. These effects are discussed in the literature [29–32].

The initial increase in electrode mass in Fig. 2 is followed by a gradual mass decrease with characteristic oscillations (Fig. 2). No doubt such mass ef-

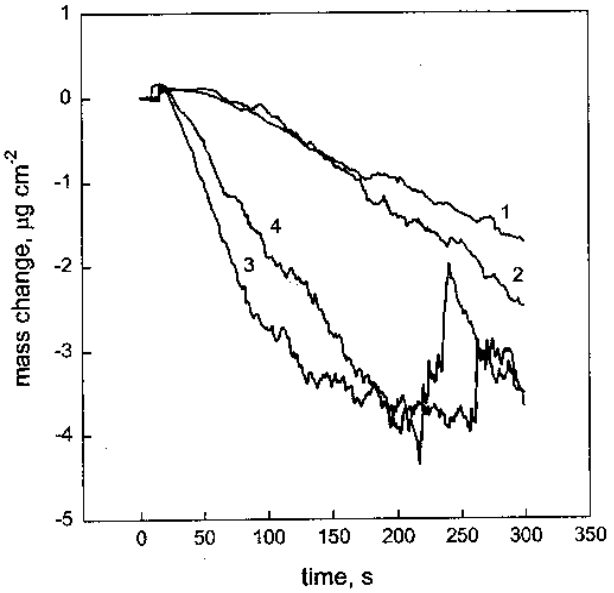

Fig. 2. Mass vs. time curves obtained at constant current polarization in metal-free solution 1.5 M Na_2SO_4 adjusted to pH 1.6. Current densities (mA cm^{-2}): *1* – 0.64; *2* – 1; *3* – 1.3; *4* – 1.9

fects are due to hydrogen evolution and, as a consequence, replacements of solution phase by gaseous one on the electrode surface.

Figure 3 depicts mass *vs*. time data obtained in the alloy plating bath when the electrode was polarized by a current step (1 mA cm^{-2}) into the region of the limiting current, where anomalous alloy deposition takes place (Fig. 1 and Table 1). The frequency-time dependence can be divided into three regions: A) rapid increase in mass, B) mass decrease, and C) the further mass growth. Assuming electrodeposition of nickel or/and zinc to be responsible

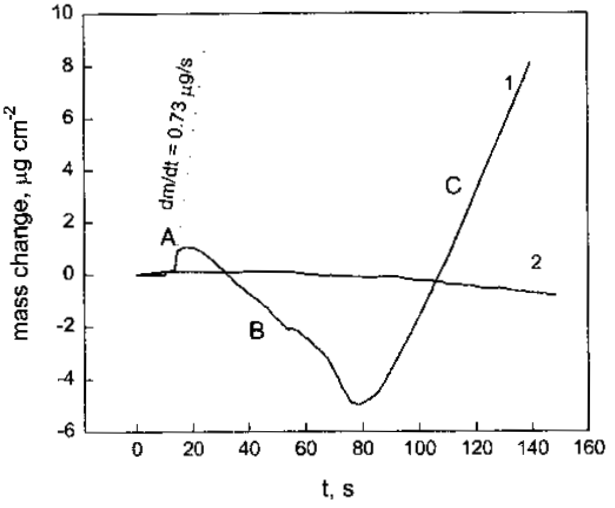

Fig. 3. Electrode mass change determined by EQCM during Zn–Ni deposition under constant current (1 mA cm^{-2}) on Au substrate (1) and under the same conditions in 1.5 M Na_2SO_4 solution adjusted to pH 1.6 (*2*)

for the initial mass increase, we can calculate according to the Faraday's law the current efficiency (b). So, the initial curve slope dm/dt = 0.73 μg/s yields b = 215% for Zn and b = 239% for Ni (the calculations for different metals give similar results, because molar masses of both metals differ only slightly). Obviously, the mass growth is much higher than predicted assuming alloy electrodeposition. We explain such behaviour by precipitation of zinc hydroxide on the electrode surface alongside any faradaic process. A pH rise due to hydrogen evolution occurs in the vicinity of the electrode after switching on the depositing current. Such increase in pH favours precipitation of hydroxides on the electrode surface. Precipitation of zinc hydroxide will be preferential, because it is less soluble than nickel hydroxide. Solubility products of both hydroxides differ by about two orders of magnitude. Since the zinc hydroxide formation has a chemical origin (not electrochemical), it may cause the mass growth higher than that predicted by Faraday's law.

The electrode mass decreases (region B, Fig. 3) when the hydroxide layer reaches its maximum thickness (m ≈ 1 μg cm^{-2}). This mass decrease is due to a prevailing hydrogen evolution, which was discussed in Fig. 2. After ca. 80 seconds of polarization the electrode mass growth starts (region C). The slope of the rectilinear part of the ascending curve is dm/dt = 0.25 μg s^{-1}, which yields b = 74% for Zn or b = 82% for Ni. Thus, we can assume that alloy deposition and hydrogen evolution take place simultaneously in region C with current efficiency b < 100%.

An analogous mass change curve was observed also when potentiostatic electrode polarization has been undertaken (Fig. 4). This figure also demonstrates that, although both blank and plating solutions are of the same pH, the current densities in the metal-free solution (curve 2) are much higher than those in the metal-containing solution (curve 1). This difference may be caused by higher overvoltage of hydrogen reduction on alloy than on gold. On the other hand, the surface blocking by hydroxide may also cause inhibition of hydrogen reduction.

Quite different mass change was observed when the electrode had been polarized into the region of normal (not anomalous) codeposition (Fig. 5, E = = –0.770 $V_{Ag/AgCl}$). There is no region B observed on the curve. Thus, hydrogen evolution in the region of normal deposition was not so extensive as in the region of anomalous deposition. It means that the conditions for hydroxide precipitation during normal deposition were less favourable, although it could not be totally disclaimed.

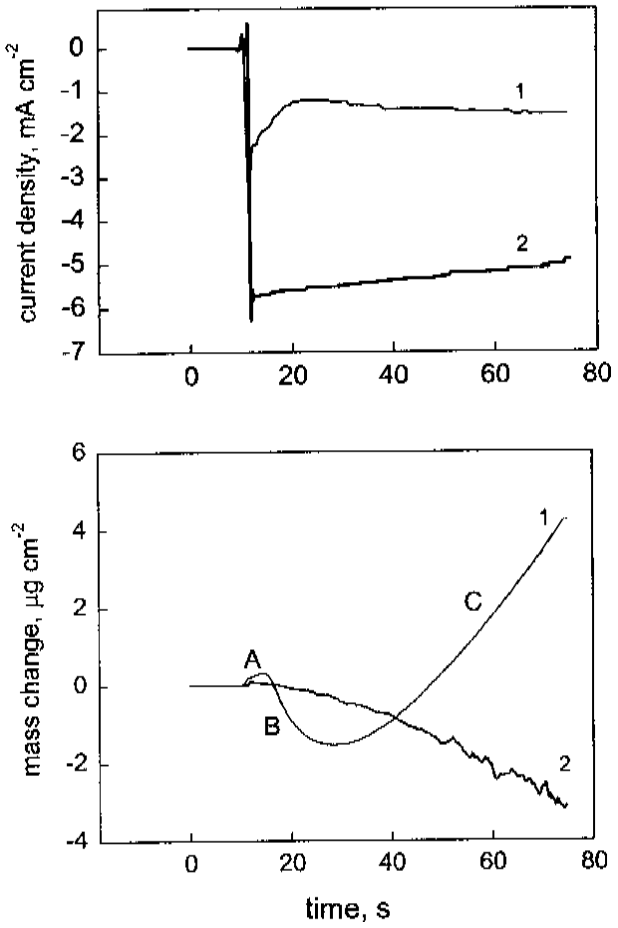

Fig. 4. Current density and electrode mass change determined by EQCM during Zn–Ni deposition under constant potential (E = –1.18 $V_{Ag/AgCl}$) on Au substrate (*1*) and under the same conditions in 1.5 M Na_2SO_4 solution adjusted to pH 1.6 (*2*)

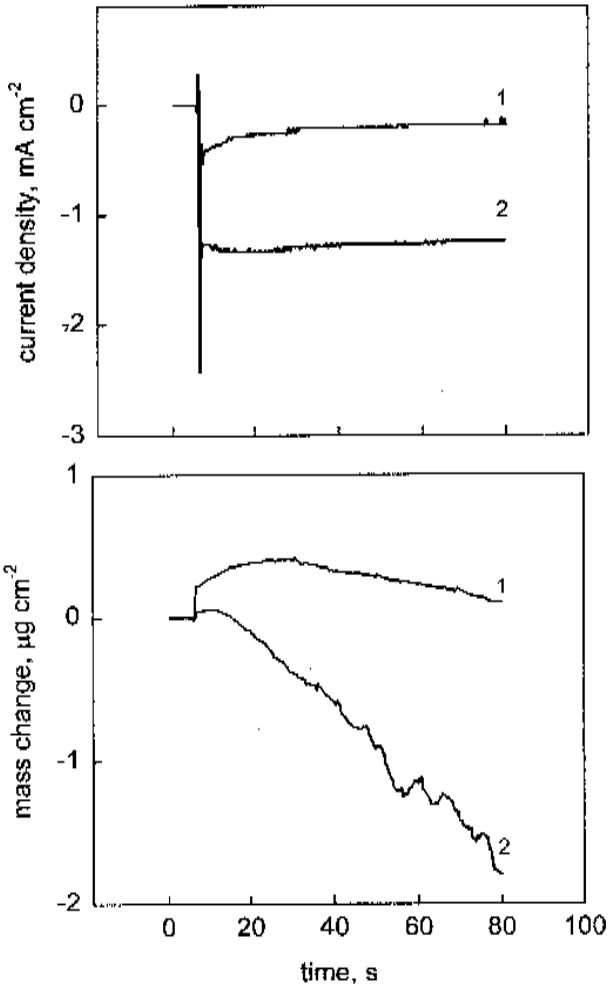

Fig. 5. Current density electrode mass change determined by EQCM during Zn–Ni deposition under constant potential (E = –0.77 $V_{Ag/AgCl}$) on Au substrate (*1*) and under the same conditions in 1.5 M Na_2SO_4 solution adjusted to pH 1.6 (*2*)

As a concluding remark, it can be noted that the EQCM data support the hydroxide suppression mechanism, which explains the anomalous Zn and Ni codeposition. It is also important to note that the obtained EQCM results harmonize with those obtained in previous investigations of anomalous Zn–Co codeposition [10]. The mass change dependencies in [10] obtained under constant current conditions exhibited also three distinctive regions and the anomalously high initial mass growth, which was explained in terms of precipitation of zinc hydroxide. Another supporting argument comes from publication [9]. The authors observed in acid sulfate solution that the mass transport influenced only normal Zn–Ni codeposition, while the transport had no influence on anomalous codeposition. Thus, it can be supposed that the rate of anomalous codeposition is determined by metal reduction from or/and through hydroxide layer, while normal codeposition is governed by diffusion laws in the solution.

CONCLUSION

The initial stages of Zn–Ni electrodeposition were investigated by electrochemical quartz crystal microbalance. The initial mass growth was much more intensive than that predicted by Faraday's law. Such behaviour was explained in terms of precipitation of scarcely soluble compounds on electrode surface. These data are in agreement with the results previously obtained for Zn–Co anomalous codeposition and support the so-called hydroxide suppression mechanism, which explains anomalous zinc codeposition with iron group metals.

Received 17 May 2001
Accepted 22 October 2001

References

1. T. Ohtsuka, A. Komori, *Electrochim. Acta,* **43,** 3269 (1998).

2. M. F. Mathias, T. W. Chapman, J. *Electrochem. Soc*., **137,** 102 (1992).
3. M. F.Mathias, T. W. Chapman, *J. Electrochem. Soc*., **134,** 1408 (1987).
4. D. Landolt, *Electrochim. Acta,* **39**, 1075 (1994).
5. Y.-P. Jin, J. R. Selman, *J. Electrochem. Soc*., **140**, 1299 (1993).
6. Y.-P. Jin and J. R. Selman, *J. Electrochem. Soc*., **140**, 1304 (1993).
7. Yu. M. Loshkarev, V. I. Korobov, V. V. Trofimenko and F. A. Chmilenko, *Protection of Metals,* **30**, 79 (1994).
8. E. Chassing and R. Wiart, *Electrochim. Acta,* **37**, (1992) 545.
9. F. J. Fabri Miranda, O. E. Barcia, S. L. Diaz, O. R. Mattos and R. Wiart, *Electrochim. Acta,* **41**, 1041 (1996).
10. A. Stankevičiūtė, K. Leinartas, G. Bikulčius, D. Virbalytė, A. Sudavičius and E. Juzeliūnas, *J. Appl. Electrochem*., *28*, 89 (1998).
11. S. S. Abd El Rehim, E. E. Fouad, S. M. Abd El Wahab and H. H. Hassan, *Electrochim. Acta,* **41**, 1413 (1996).
12. H. Yan, J. Downes, P. J. Boden and S. J. Haris, *J. Electrochem. Soc.,* **143**, 1577 (1996).
13. H. M. Wang, T. J. O' Keefe, J. Appl. Electrochem., **24**, 900 (1994).
14. Zh. Wu, L. Fedrizzi and P. L. Bonora, *Surf. Coat. Technol*., **85**, 170 (1996).
15. M. A. Pech-Canul, R. Ramanauskas and L. Maldonado, *Electrochim. Acta,* **42**, 255 (1997).
16. A. M. Alfantazi, J. Page and U. Erb. *J. Appl. Electrochem*., **26**, 1225 (1996).
17. M. Pushpavanam and K. Balakrishnan, *J. Appl. Electrochem*., **26**, 283 (1996).
18. M. Pushpavanam, K. Balakrishnan, *J. Appl. Electrochem*., **26**, 1065 (1996).
19. T. Oki, M. M. Younan, *Galvanotechnik,* **87**, 1131 (1996).
20. A. M. Alfantazi and U. Erb, *Corrosion,* **52**, 880 (1996).
21. R. Fratesi and G. Roventi, *J. Appl. Electrochem*., **22**, 657 (1992).
22. M. J. Nicol and H. I. Philip, *J. Electroanal. Chem*., **70**, 233 (1976).
23. H. Dahms and I. M. Croll, *J. Electrochem. Soc*., **112**, 771 (1965).
24. K. Higashi, H. Fukushima, T. Urakuwa, T. Adania and K. Matsudo, *J. Electrochem. Soc*., **128**, 2081 (1981).
25. H. Fukushima, T. Akiyama, K. Higashi, R. Kammel and M. Karimkhani, *Metall,* **42**, 242 (1988).
26. H. Fukushima, T. Akiyama, K. Higashi, R. Kammel and M. Karimkhani, *Metall,* **44**, 754 (1990).
27. G. Sauerbrey, *Z. Phys*., **155**, 206 (1959).
28. E. Juzeliūnas, P. Kalinauskas and P. Miečinskas. *J. Electrochem. Soc.,* **143**, 1525 (1996).
29. R. Schumacher, Angew. *Chem*., **102**, 347 (1990).
30. W. Stöckel, and R. Schumacher, *Ber. Bunsen Ges. Phys. Chem*., **91**, 345 (1987).
31. E. Juzeliūnas and K. Jüttner, *Electrochim. Acta,* **43**, 1691 (1998).
32. E. Juzeliūnas, H.Pickering and K. G. Weil, *J. Electrochem., Soc*. **147**, 1088 (2000).

R. Valotkienė, K. Leinartas, D. Virbalytė, E. Juzeliūnas

ANOMALAUS ZN–NI SĄSĖDŽIO SULFATINIAME ELEKTROLITE TYRIMAS EQCM METODU

S a n t r a u k a

Atlikti sistemos Zn–Ni pradinių sąsėdžio stadijų mikrogravimetriniai tyrimai. Nustatytos masės pokyčio priklausomybės, esant pastoviai srovei arba pastoviam potencialui, parodė, kad yra trys charakteringos zonos: 1) pradinis masės augimas, kuris daug didesnis negu apskaičiuotas pagal Faradėjaus dėsnį. Jį galima paaiškinti hidroksidų susidarymu ant paviršiaus; 2) masės sumažėjimas dėl vandenilio skyrimosi; 3) tiesialinijinis masės augimas dėl lydinio nusėdimo. Tokia elgsena paaiškinta hidroksidinio slopinimo mechanizmu, paaiškinančiu ir anomalų Zn sąsėdį su geležies grupės metalais. Duomenys atitinka sistemos Zn–Co anomalaus sąsėdžio dėsningumus, anksčiau gautus kvarco kristalo mikrogravimetrijos metodu.

Р. Валоткене, К. Лейнартас, Д. Вирбалите, Э. Юзелюнас

ИССЛЕДОВАНИЕ АНОМАЛЬНОГО СООСАЖДЕНИя ZN–NI В СУЛЬФАТНОМ ЭЛЕКТРОЛИТЕ МЕТОДОМ ЭКМ

Р е з ю м е

Методом электрохимических кварцевых микровесов исследованы начальные стадии соосаждения системы Zn–Ni. Зависимости изменения массы, установленные при постоянном токе или постоянном потенциале, показали три характерные зоны: 1) начальное увеличение массы, намного больше чем рассчитанное по закону Фарадея, что объясняется формированием оксида на поверхности, 2) уменьшение массы из-за выделения водорода, 3) прямолинейный рост массы из-за осаждения сплава. Такое в победение объясняет механизм гидроксидного торможения, в свою очередь объясняющий аномальное соосаждение Zn с металлами группы железа. Результаты соответствуют закономерностям аномального соосаждения системы Zn-Co, полученным ранее методом ЭКМ.